Supporting Reference 2

Accelerated Publication

THE JOURNAL OF BIOLOGICAL CHEMISTRY
Vol. 277, No. 21, Issue of May 24, pp. 18245–18248, 2002

Engineering-enhanced Protein Secretory Expression in Yeast with Application to Insulin*[S]

Received for publication, March 7, 2002,
and in revised form, March 27, 2002
Published, JBC Papers in Press, March 28, 2002,
DOI 10.1074/jbc.C200137200

Thomas Kjeldsen‡, Svend Ludvigsen, Ivan Diers, Per Balschmidt, Anders R. Sørensen, and Niels C. Kaarsholm

From the Novo Nordisk A/S, Novo Alle, DK-2880 Bagsvaerd, Denmark

Adaptation to efficient heterologous expression is a prerequisite for recombinant proteins to fulfill their clinical and biotechnological potential. We describe a rational strategy to optimize the secretion efficiency in yeast of an insulin precursor by structure-based engineering of the folding stability. The yield of a fast-acting insulin analogue (Asp^{B28}) expressed in yeast was enhanced 5-fold by engineering a specific interaction between an aromatic amino acid in the connecting peptide and a phenol binding site in the hydrophobic core of the molecule. This insulin precursor is characterized by significantly enhanced folding stability. The improved folding properties enhanced the secretion efficiency of the insulin precursor from 10 to 50%. The precursor remains fully *in vitro* convertible to mature fast-acting insulin.

Administration of the two-chain 51-amino acid peptide hormone insulin is life sustaining for many of the 150 million diabetic patients in the world. Classical pancreatic extraction results in 10–15 mg of insulin per pancreas and the number of porcine or bovine pancreases to produce current requirements of insulin (in excess of 7 metric tons) is simply not available. Consequently, a substantial fraction of insulin is today produced by eukaryotic secretory expression in the yeast *Saccharomyces cerevisiae*. Recently, second generation fast-acting genetically engineered insulin analogues have been engineered for improved diabetes therapy. This is exemplified by the clinically relevant fast-acting insulin, which features an amino acid substitution in position 28 of the B-chain from proline to aspartic acid and is used for treatment of diabetes mellitus (1).

However, many biochemical and structural properties of insulin and proinsulin have evolved in response to differential requirements of biosynthesis, processing, transport, and storage in the β-cells of Langerhans islets (2, 3). Importantly, insulin and insulin analogues are readily adapted for expression in yeast as single-chain proinsulin-like precursors lacking the connecting peptide in the following configuration: amino acid residues 1–29 of the B-chain connected to the A-chain by a short removable mini-C-peptide and fused to the yeast prepro-α factor through a single dibasic cleavage site (secretory expression of insulin in yeast and *in vitro* enzymatic conversion of the precursor to insulin has recently been reviewed (4, 5)). Removal of the prepro-α factor by endoproteolytic cleavage by the Kex2 endoprotease in a late Golgi compartment generates a single-chain insulin precursor with self-association properties and structure essentially similar to that of human two-chain insulin (6, 7).

Proteins exit the lumen of the endoplasmic reticulum (ER)[1] after folding, and frequently this is a rate-limiting step in secretion (8–10). Herein we describe an improvement in eukaryotic secretion efficiency with application to insulin, using a strategy of structure-based rational engineering under the assumption that a more stably folded precursor molecule is accompanied by more efficient transport through the secretory pathway. The structure of the Asp^{B28} insulin precursor, termed insulin aspart, as a hexamer and its binding sites for small molecule ligands (11) are used to develop novel C-peptides tailored to provide structural stability to the precursor molecule. The resulting enhancement of the expression yield correlated with increased structural stability and is rationalized in terms of the structure of the novel precursor molecule.

EXPERIMENTAL PROCEDURES

General Molecular Biology Techniques—Materials, strains, media, and general molecular biology techniques and yeast expression were as described previously unless otherwise mentioned (12–14). Expression of insulin precursors in *S. cerevisiae* was performed in the following configuration: α-factor leader-KR-spacer-insulin precursor, where KR is the Kex2 dibasic endoprotease processing site. To optimize processing of the fusion protein by the *S. cerevisiae* Kex2 endoprotease, a spacer peptide, EEAEAEAPK, was present between the leader and the insulin precursor (13). The mature insulin precursor was secreted as a single-chain N-terminally extended proinsulin-like polypeptide with a short synthetic peptide connecting Lys^{B29} and Gly^{A1}. After purification of the insulin precursor and proteolytic removal of the N-terminal extension and connecting peptide, the amino acid Thr^{B30} can be added to Lys^{B29} by trypsin-mediated transpeptidation to generate insulin (15).

Quantification and Purification of Insulin Precursors—Quantification of the insulin aspart precursor yield in the culture supernatants was performed as previously described (12, 16). Pulse-chase analysis employed 2.5-min metabolic labeling with [^{35}S]cysteine using cultures with an A_{600} of ~10 as previously described (12). The insulin precursor was captured from acidified and clarified culture supernatant by adsorption to a cation exchange column. The eluted protein was further purified by preparative reverse phase high pressure liquid chromatography on a C18 silica column with an ethanol/water gradient in phosphate buffer at pH 3. The main protein peak was collected and finally lyophilized after desalination.

Guanidine Hydrochloride (GdnHCl)-induced Protein Denaturation—The GdnHCl-induced unfolding was measured by far-UV CD using a Jasco J-715 spectropolarimeter at pH 8.0 as described (17). The unfolding curves display the relative change in CD at 224 nm $(\Delta\epsilon_{obsd} - \Delta\epsilon_{base})/-\Delta\epsilon_{base}$ as a function of denaturant concentration, where $\Delta\epsilon_{base}$ is the observed CD in the (horizontal) pre-transition zone. For each precursor, C_{mid} is the concentration of GdnHCl corresponding to unfolding of one-half of the population.

NMR Spectroscopy—NMR spectra were recorded at 600 and 800

* The costs of publication of this article were defrayed in part by the payment of page charges. This article must therefore be hereby marked "*advertisement*" in accordance with 18 U.S.C. Section 1734 solely to indicate this fact.

[S] The on-line version of this article (available at *http://www.jbc.org*) contains a supplemental table.

‡ To whom correspondence should be addressed: Insulin Research, Novo Nordisk A/S, Novo Alle, DK-2880 Bagsvaerd, Denmark. Tel.: 45-44423022; Fax: 45-44444256; E-mail: thk@novonordisk.com.

[1] The abbreviations used are: ER, endoplasmic reticulum; GdnHCl, guanidine hydrochloride; NOESY, two-dimensional nuclear Overhauser enhanced spectroscopy; NOE, nuclear Overhauser enhancement.

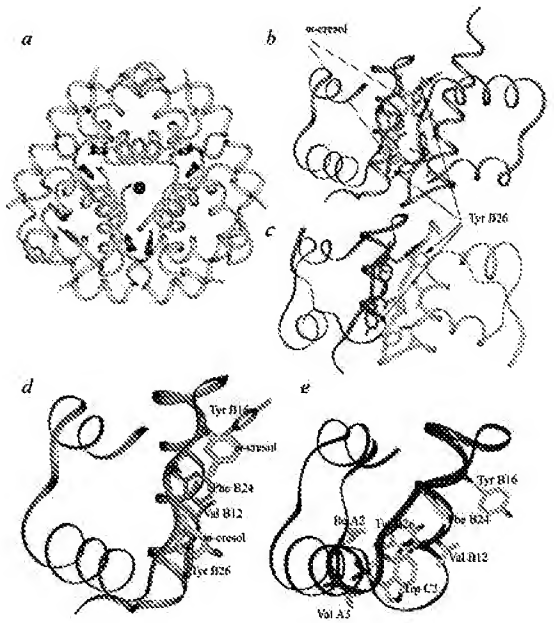

FIG. 1. The hexamer structure (*a*) of insulin aspart precursor^{AAK} (Protein Data Bank code 1ZEI) determined by x-ray crystallography (11) has two unique binding sites (shown in *blue*) for *m*-cresol in the third dimer of insulin aspart precursor^{AAK} hexamer, in addition to the classical insulin *m*-cresol/phenol binding sites (shown in *red*). The two extra *m*-cresol molecules are inserted between the monomers in almost symmetrically equivalent binding sites (*b*), which are composed of residues Tyr^{B26} and Val^{B12} from one monomer and Leu^{B15}, Tyr^{B16}, Cys^{B19}, and Phe^{B24} from the second monomer of the dimer. For comparison of the insulin aspart precursor^{AAK} dimer structure with the classical insulin dimer structure, see *panel c*). In solution, at monomeric conditions without *m*-cresol present, the tryptophan side chain in the engineered mini-C-peptide binds to the *m*-cresol binding site (in a slightly shifted position), thus providing an anchor point for the elongated A1-helix (*e*). This aromatic amino acid binding pocket in the insulin aspart precursor^{EWK} is comparable with the *m*-cresol binding pocket found in the crystal state of the insulin aspart precursor^{AAK} (*d*).

MHz using a Varian Inova. Procedures for sample preparation at pH 8, spectral recording, and assignment as well as methods for determination of three-dimensional structures have been described recently (Ref. 18, and references cited therein).

RESULTS AND DISCUSSION

Engineering the Insulin Aspart Precursor to High Yield Yeast Secretory Expression—Binding of phenol to the insulin hexamer causes well described classical allosteric conformational changes, *i.e.* the $T_6 \rightarrow T_3R_3 \rightarrow R_6$ transformations (6, 19, 20). The R_6 hexameric crystal structure of the insulin aspart precursor^{AAK} (for simplicity the sequence of the mini-C-peptide is indicated in superscript) (Protein Data Bank code 1ZEI) has a number of unique features compared with the classical R_6 insulin hexamer (11). The monomers, which comprise the hexamer, are composed of traditional structural elements common to the R-state insulin, *i.e.* an α-helix (B1–B19), a turn (B20–B23), one-half anti-parallel β-sheet (B24–B28), and a loop (B29–C1) (Fig. 1). The A-chain is composed of a slightly extended A1 α-helix (C2–C3, A1–A9), a loop (A10–A13), and finally the A2 α-helix (A14–A20). Besides the classical phenol or *m*-cresol binding sites, one of the three dimers has two additional *m*-cresol molecules located in the monomer-monomer interface next to Tyr^{B26} (Fig. 1). These two binding sites are essentially identical and composed by the hydrophobic residues Tyr^{B26} and Val^{B12} from one monomer and Leu^{B15}, Tyr^{B16}, Cys^{B19}, and Phe^{B24} of the other monomer molecule (Fig. 1).

It has been shown that folding stability is important for secretion efficiency (5, 8–10). We hypothesized that the side chain of an aromatic amino acid localized in the mini-C-peptide will mimic the interactions provided by the *m*-cresol ligand shown in Fig. 1. Importantly, the interaction of this hydrophobic residue with the hydrophobic core of the molecule would be energetically favorable and presumably enhance the folding stability of the precursor. The precursor can be converted into the mature two-chain insulin aspart by *in vitro* enzymatic removal of the C-peptide, which restores full biological potential of the molecule.

TABLE I

Yeast expression yield and folding stability of insulin precursors

The expression yield was determined as described under "Experimental Procedures" and normalized for comparison to the yield of the insulin aspart precursor^{AAK}. Folding stability of the precursors is described as C_{mid}, the concentration of GdnHCl corresponding to unfolding of one-half the population. C_{mid} is derived from Fig. 3. ND, not determined. The insulin precursor comprising the first 29 amino acids of the insulin B-chain joined to the 21 amino acids of the insulin A-chain either by a C-peptide or directly as indicated and expressed in *S. cerevisiae* as described under "Experimental Procedures."

Insulin precursor amino acid substitution	C-peptide	Relative yield	C_{mid}
			M
Asp^{B28}	AAK	1.0	5.2
Asp^{B28}		1.2	5.6
Asp^{B28}	EWK	4.9	7.2
Asp^{B28}	EYK	3.8	ND
Asp^{B28}	EFK	3.5	ND
Asp^{B28}	LWK	3.6	6.4
Glu^{B10}, Asp^{B28}, His^{A8}, Glu^{A14}		5.3	7.0
Glu^{B10}, Asp^{B28}, His^{A8}, Glu^{A14}	EWK	7.6	>7.9

Introduction of an aromatic amino acid into the mini-C-peptide, *e.g.* EWK, did indeed increase the expression yield of the insulin aspart precursor (Table I). Tryptophan had the greatest positive influence (5-fold) on the expression yield, whereas phenylalanine and tyrosine increase the expression yield ~3.5-fold (Table I). Mini-C-peptides with various amino acids in combination with the aromatic amino acid, *e.g.* LWK, enhanced the expression yield of the insulin aspart precursor (Table I). Interestingly, the position of the aromatic amino acid in the mini-C-peptide influenced the expression yield of the insulin aspart precursor. When the aromatic amino acid is in an N-terminal position to the lysine in the mini-C-peptide the secretion efficiency of the insulin aspart precursor is increased. Exchanging the sequence of the mini-C-peptide to WEK or shortening the mini-C-peptide to WK did not significantly increase the expression yield of the insulin aspart precursor. The significance of the position of tryptophan indicates that a specific molecular interaction mediates the increase in the secretion efficiency of the insulin aspart precursor.

The effect of an aromatic acid in the mini-C-peptide (EWK) on the secretion of the insulin aspart precursor expressed in yeast was further investigated by pulse-chase analysis with a 2.5-min pulse with [^{35}S]cysteine followed by 30 min of chase. The quantity of insulin aspart precursor with the EWK mini-C-peptide synthesized after the [^{35}S]cysteine pulse is substantially larger than the quantity of precursor synthesized with the AAK mini-C-peptide (only the insulin aspart precursor is labeled) (Fig. 2). Furthermore, the quantity of the insulin aspart precursor^{EWK} secreted to the culture supernatant after 30 min of chase was six times higher than with the AAK mini-C-peptide. Interestingly, a similar quantity of synthesized insulin aspart precursor was retained intracellularly in the vacuole independent of the mini-C-peptide. However, the insulin aspart precursor^{EWK} was more efficiently secreted (Fig. 2). The secretion efficiency of the insulin aspart precursor^{EWK} is illustrated by the ratio of secreted precursor increased from 10 to 50% (Fig. 2).

Folding Stability of Insulin Aspart Precursors—To evaluate

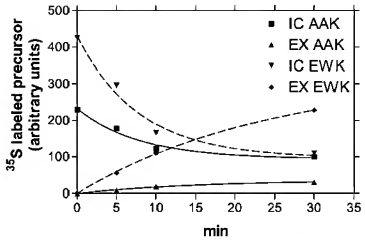

FIG. 2. **Secretion of the insulin aspart precursor with either the AAK C-peptide or the EWK C-peptide expressed in *S. cerevisiae* analyzed by pulse-chase analysis.** The *S. cerevisiae* cells were pulsed for 2.5 min with [^{35}S]cysteine and subsequently chased for 0, 5, 10, or 30 min with an excess of unlabeled cysteine. After the pulse-chase experiment, proteins were separated by SDS-PAGE and quantified by PhosphorImager analysis (Molecular Dynamics). The secretion kinetic of the insulin aspart precursor with the AAK mini-C-peptide is shown as a *solid line* and with the EWK mini-C-peptide as a *dashed line*. Insulin aspart precursor localized intracellularly (*IC*) is indicated by ▼ and ■ and extracellularly (*EX*) by ▲ and ♦. The data summarize labeled precursor both as fusion protein and as mature precursor (only the precursor was labeled), and the data were normalized for comparison using endogenous protein as internal standard.

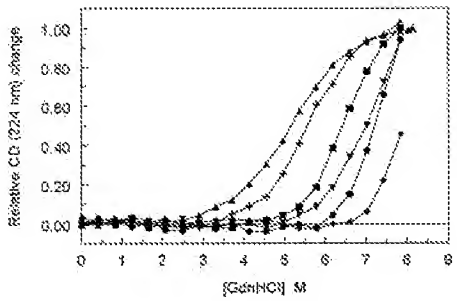

FIG. 3. **Unfolding curves for native and mutant insulin precursors expressed as the relative change in CD at 224 nm as a function of GdnHCl concentration.** ▲, insulin aspart precursor^{AAK}; +, insulin aspart precursor^{-} (minus indicates a direct connection between B29 and A1); ■, insulin aspart precursor^{LWK}; ▼, insulin aspart precursor^{-} with the additional amino acid substitutions Glu^{B10}, Asp^{B28}, His^{A8}, and Glu^{A14}; ●, insulin aspart precursor^{EWK}; and ♦, insulin aspart precursor^{EWK} with the additional amino acid substitutions Glu^{B10}, Asp^{B28}, His^{A8}, and Glu^{A14}. The insulin aspart precursors, except insulin aspart precursor^{AAK}, featured a N-terminal extension with the sequence E(EA)$_3$PK that improved Kex2 endoprotease processing during secretion (see "Experimental Procedures" for further details).

whether the improved secretion of insulin aspart precursors reflected improved folding, the precursors were purified and the *in vitro* folding stability determined. The *in vitro* folding stability of the precursors was assessed by titrations with the protein denaturant GdnHCl and detection by far-UV CD spectroscopy. The far-UV CD as a function of increasing concentrations of GdnHCl monitors the loss of secondary structure that accompanies protein unfolding. As shown in Fig. 3, the introduction of EWK and LWK mini-C-peptides strongly enhances the folding stability of the insulin aspart precursor. These data suggest that the *in vitro* folding stability is positively correlated with expression yield. To further investigate this correlation, additional amino acid substitutions, Glu^{B10}, His^{A8}, Glu^{A14}, were introduced to stabilize the α-helices of the insulin aspart precursor with and without the EWK mini-C-peptide (see Ref. 17 for design of helix capping). The helix-capping substitutions enhanced the folding stability and concomitantly increased the expression yield of the precursor 4.2-fold (Table I). Moreover, the combination of the EWK mini-C-peptide and these amino acid substitutions further improved the folding stability of the precursor, and the expression yield was increased 7.6-fold relative to the insulin aspart precursor^{AAK} (Table I). Indeed, the combination of the EWK mini-peptide and the α-helix capping mutations results in an insulin species that remains essentially folded at 7 M GdnHCl. This corresponds to about a 200-fold shift in the forms in favor of the folded state in comparison with the insulin aspart precursor^{AAK} species. Thus, the folding stability is a principal parameter in determining eukaryotic secretion efficiency. The previously described natural and synthetic C-peptides of insulin appear to offer little structural support or interaction with the remainder of the molecule. In contrast, the C-peptides described here have significant impact on the overall structure of the molecule by both intramolecular interaction and a direct contribution to the structural elements of the precursor.

The activities of human insulin and insulin aspart are similar when determined by both metabolic potency (lipogenesis) and by receptor affinity (21). However, the single-chain insulin precursor has ~0.1% activity of the two-chain mature molecules (22). This has been interpreted that flexibility in the C terminus of the B-chain and a free N terminus of the A-chain are required for activity (22, 23). The activity (lipogenesis) of the described single chain insulin aspart precursor featuring tryptophan in the C-peptide is further decreased 10-fold to ~0.01% of human insulin. The low activity of this precursor is consistent with decreased flexibility in the C terminus of the B-chain and the N terminus of the A-chain because this region has been anchored by the tryptophan to the hydrophobic core of the molecule. Importantly, *in vitro* conversion of the insulin aspart precursors to the two-chain insulin aspart molecule restores full activity to the mature two-chain molecule (21).

Tertiary Structure of the Insulin Aspart Precursor—To assess the structural mechanism behind the concomitantly improved secretion and folding stability, the structure of the insulin aspart precursor was determined. The structure of the insulin aspart precursor^{EWK} was determined by NMR spectroscopy based on two-dimensional proton NMR spectra at pH 8.0 and 1.0 mM. At these conditions the precursor does not dimerize or otherwise self-associate to any significant degree. Structure elucidation of the insulin aspart precursor^{EWK} from NMR data agrees with other structures determined by similar methods (see supplementary table). The two-dimensional NOESY spectra of the insulin aspart precursor^{EWK} are significantly different from similar spectra of the insulin aspart precursor^{AAK} (data not shown).

The structure of the insulin aspart precursor^{EWK} (Fig. 4) shares secondary structural elements with other insulin structures (24) including the extended structure from B1–B8, the α-helix B9–B19, a turn B20–B23, and a half-β-sheet structure from B24 to B27. However, the EWK mini-C-peptide and especially Trp^{C2} induce a number of distinct structural differences compared with all previously described insulin structures (Figs. 1 and 4). Importantly, Trp^{C2} is partly inserted into the binding site that is described above, which binds *m*-cresol/phenol in the insulin aspart precursor^{AAK} (Fig. 1). The tryptophan side chain moiety packs against Ile^{A2} and Val^{A3} as its helical neighbors to Leu^{B11}, Val^{B12}, and Leu^{B15} in the central B-chain helix and in the C-terminal part of the B-chain to Tyr^{B26} and Asp^{B28}. Furthermore, Tyr^{B26} together with Asp^{B28} have been rearranged to open the *m*-cresol binding site to Trp^{C2} (Fig. 4).

Furthermore, the insertion of the tryptophan into the hydrophobic core results in a re-orientation of the half-β-sheet structure from B24 to B27 and extension of the A1 α-helix of the A-chain (Fig. 4). The two-dimensional NOESY spectra of the insulin aspart precursor^{EWK} show an extensive number of NOEs indicative of an α-helix from C2–A8. However, these NOEs are almost absent in the spectra of insulin aspart precursor^{AAK}. Furthermore, the chemical shift values of α-protons assigned for residues of the insulin aspart precursor^{EWK} in this

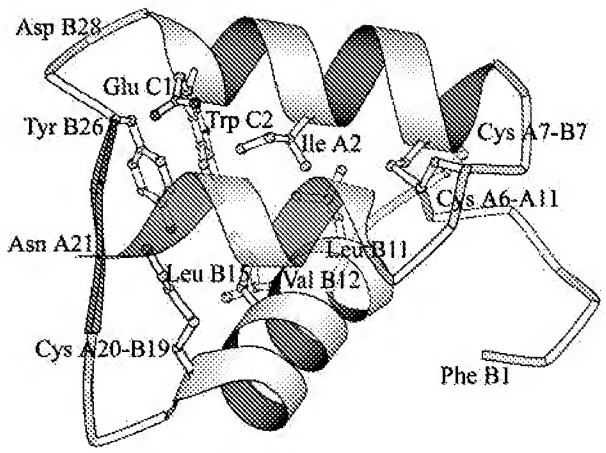

FIG. 4. **Schematic representation of insulin aspart precursor^{EWK} structure as determined by NMR displayed using Molscript (26).** The second A-chain helix is semi-transparent to allow visualization of the interaction of Trp^{C2} to its structural neighbors shown in stick representation. Besides NOEs to the sequentially neighboring residues, tryptophan^{C2} has several NOEs to residues Ile^{A2}, Val^{A3}, LeuB11, Val^{B12}, Leu^{B15}, Tyr^{B26}, and Asp^{B28}. The residues with NOEs to Trp^{C2} form a hydrophobic cleft almost equivalent to the *m*-cresol binding pocket described in the insulin aspart precursor^{AAK} structure by x-ray crystallography (11) (see text for details).

region are on average shifted 0.35 up-field (lower ppm value) supporting that the residues of the EWK mini-C-peptide and the five first residues in the A-chain of the insulin aspart precursor^{EWK} reside in an α-helical structure. Interestingly, the x-ray-derived structure of the insulin aspart precursor^{AAK} also indicates an α-helix from C2–A8 (11). We conclude that the enhanced folding stability originates from the extended A-chain helix, which is anchored to the molecule by hydrophobic packing of the tryptophan side chain.

Moreover, the half-β-sheet structure from B24 to B27 is moved further away from the center of the molecule compared with other insulin structures. The residues B28, B29, and C1 form a small ill defined coil structure, which is the starting point of the well defined α-helix from C2 to A8. This structural re-organization of the C-terminal part of the B-chain accommodates both the extension of the A1 α-helix and the insertion of the tryptophan residue side chain into the hydrophobic core of the molecule (Fig. 4).

A novel aspect of the present studies is that structural improvement of molecular stability concomitantly enhances the efficiency whereby insulin traffics through the eukaryotic secretory pathway. Moreover, the enhanced folding stability was engineered by a hydrophobic interaction based on a specific phenol binding site in the core of the molecule. Furthermore, this intramolecular interaction introduces unique structural elements into the insulin molecule. Thus, the expressed molecule is not a mutant version of fast-acting insulin but a rational structurally adapted precursor that is readily converted into the native, two-chain structurally identical fast-acting insulin. Intriguingly, it was possible to further enhance the secretion efficiency in a synergistic manner by combing this novel stabilizing intramolecular interaction with more classical stabilization of the secondary structure elements. Interestingly, it has been shown that mutants of bovine pancreatic trypsin inhibitor with impaired folding properties also were expressed inefficiently in yeast (9, 10). This was interpreted that the thermodynamic stability can determine the efficiency of escape from ER, presumably because of degradation of inefficiently folded molecules. However, it has also been shown that insulin expressed in a *sec*18–1 mutant yeast strain, where the molecule cannot reach the Golgi complex, is not degraded, strongly indicating that insulin is not subjected to ER-associated degradation in yeast (25). The presented data support a model where the structural and folding properties of the insulin molecule are key factors for efficient biosynthesis and secretion.

Acknowledgments—Excellent technical assistance was provided by Annette Frost Pettersson, Kate Müggler, Ane Blom, Susan E. Danielsen, Heidi Green, and Lene Villadsen. Access to the "Danish Instrument Centre for NMR Spectroscopy of Biological Macromolecules" 800-MHz NMR instrument at Carlsberg Laboratory is highly appreciated.

REFERENCES

1. Brange, J., Ribel, U., Hansen, J. F., Dodson, G., Hansen, M. T., Havelund, S., Melberg, S. G., Norris, F., Norris, K., Snel, L., Sørensen, A. R. & Voigt, H. O. (1988) *Nature* **333,** 679–682
2. Blundell, T. L., Cutfield, J. F., Cutfield, S. M., Dodson, E. J., Dodson, G. G., Hodgkin, D. C., Mercola, D. A. & Vijayan, M. (1972) *Nature* **231,** 506–511
3. Dodson, G. & Steiner, D. F. (1998) *Curr. Opin. Struct. Biol.* **8,** 189–194
4. Kjeldsen, T. (2000) *Appl. Microbiol. Biotechnol.* **54,** 277–386
5. Kjeldsen, T., Balschmidt, P., Diers, I., Hach, M., Kaarsholm, N. C. & Ludvigsen, S. (2001) *Biotechnol. Genet. Eng. Rev.* **18,** 89–121
6. Kaarsholm, N. C., Ko, H-C. & Dunn, M. F. (1989) *Biochemistry* **28,** 4427–4435
7. Derewenda, U., Derewenda, Z., Dodson, E. J., Dodson, G. G., Bing, X. & Markussen, J. (1991) *J. Mol. Biol.* **220,** 425–433
8. Ellgaard, L., Molinari, M. & Helenius, A. (1999) *Science* **286,** 1882–1888
9. Kowalski, J. M., Parekh, R. N., Mao, J. & Wittrup, K. D. (1998) *J. Biol. Chem.* **273,** 19453–19458
10. Kowalski, J. M., Rajesh, N., Parekh, R. N. & Wittrup, K. D. (1998) *Biochemistry* **37,** 1264–1273
11. Whittingham, J. L., Edwards, D. J., Antson, A. A., Clarkson, J. M. & Dodson, G. G. (1998) *Biochemistry* **37,** 11516–11523
12. Kjeldsen, T., Pettersson, A. F. & Hach, M. (1999) *J. Biotechnol.* **75,** 195–208
13. Kjeldsen, T., Brandt, J., Andersen, A. S., Egel-Mitani, M., Hach, M., Pettersson, A. F. & Vad, K. (1996) *Gene (Amst.)* **170,** 107–112
14. Kjeldsen, T., Pettersson, A. F., Hach, M., Diers, I., Havelund, S., Hansen, P. H. & Andersen, A. S. (1997) *Protein Expression Purif.* **9,** 331–336
15. Markussen, J., Damgaard, U., Diers, I., Fiil, N., Hansen, M. T., Larsen, P., Norris, F., Norris, K., Schou, O., Snel, L., Thim, L. & Voigt, H. O. (1987) in *Peptides 1986* (Theodoropoulos, D., ed) pp. 189–194, Walter de Gruyter & Co., Berlin
16. Snel, L. & Damgaard, U. (1988) *Horm. Metab. Res.* **20,** 476–488
17. Kaarsholm, N. C., Norris, K., Jørgensen, R. J., Mikkelsen, J., Ludvigsen, S., Olsen, H. B., Sørensen, A. R. & Havelund, S. (1993) *Biochemistry* **32,** 10773–10778
18. Ludvigsen, S., Thim, L., Blom, A. M. & Wulff, B. S. (2001) *Biochemistry* **40,** 9082–9088
19. Derewenda, U., Derewenda, Z., Dodson, E. J., Dodson, G. G., Reynolds, C. D., Smith, G. D., Sparks, C. & Swenson, D. (1989) *Nature* **338,** 594–596
20. Bloom, C. R., Choi, W. E., Brzovic, P. S., Ha, J. J., Huang, S.-T., Kaarsholm, N. C. & Dunn, M. F. (1995) *J. Mol. Biol.* **245,** 324–330
21. Kurtzhals, P., Schäffer, L., Sørensen, A., Kristensen, C., Jonassen, I., Schmid, S. & Trüb, T. (2000) *Diabetes* **49,** 999–1005
22. Markussen, J., Jørgensen, K. H., Sørensen, A. R. & Thim, L. (1985) *Int. J. Pept. Protein Res.* **26,** 70–77
23. Nakagawa, S. H. & Tager, H. S. (1992) *Biochemistry* **31,** 3204–3214
24. Ludvigsen, S., Roy, M., Thøgersen, H. & Kaarsholm, N. C. (1994) *Biochemistry* **33,** 7998–8006
25. Zhang, B-Y., Chang, A., Kjeldsen, T. & Arvan, P. (2001) *J. Cell Biol.* **153,** 1187–1198
26. Kraulis, P. J. (1991) *J. Appl. Crystallogr.* **24,** 946–950
27. Laskowski, R. A., Rullmann, J. A. C., Macarthur, M. W., Kaptein, R. & Thornton, J. M. (1996) *J. Biomol. NMR* **8,** 477–486